

# Broadband fast semiconductor saturable absorber

G. R. Jacobovitz-Veselka and U. Keller

*AT&T Bell Laboratories, Crawford Corner Road, Holmdel, New Jersey 07733*

M. T. Asom

*AT&T Bell Laboratories, Route 222, Breinigsville, Pennsylvania 18031*

Received July 21, 1992

Kerr lens mode-locked (KLM) solid-state lasers are typically not self-starting. We address this problem by introducing a broadband semiconductor saturable absorber that could be used as a tunable, all-solid-state, passive starting mechanism. We extend the wavelength tunability of a semiconductor saturable absorber to more than 100 nm using a band-gap-engineered low-temperature molecular-beam-epitaxy (MBE)-grown bulk AlGaAs semiconductor saturable absorber in which the absorption edge of the saturable absorber has been artificially broadened by continuously reducing the Al concentration during the MBE growth. We demonstrate its tunability and its feasibility as a starting mechanism for KLM with a picosecond resonant passive mode-locked Ti:sapphire laser. The extension to femtosecond KLM lasers has been discussed previously.

Recent advances in ultrafast pulse generation with solid-state lasers opened up a new era in femtosecond laser technology.<sup>1,2</sup> Sub-100-fs tunable pulses are now commercially available with Kerr lens mode-locked (KLM) Ti:sapphire lasers. The mode-locking nonlinearity is based on the Kerr effect, which, when combined with an intracavity aperture, forms an effective saturable absorber. Because the Kerr effect scales with the peak intensity, cw lasing fluctuations alone are not sufficient to start and sustain KLM operation. Therefore different methods have been used to start the KLM laser such as higher-order mode beating noise (from a slightly misaligned laser),<sup>2</sup> weak resonant passive mode locking<sup>3</sup> (RPM), a weak intracavity dye absorber,<sup>1,4</sup> active modulators,<sup>5</sup> synchronous pumping,<sup>6</sup> and moving mirrors.<sup>7</sup> By using different kinds of starting mechanism, new short-pulse records have been published nearly monthly with the shortest pulse duration currently at 17 fs.<sup>8</sup>

Aside from the excitement of ever-shorter pulses, a simple, reliable, all-solid-state-based and possibly passive starting mechanism is still required. The need for such a simple starting mechanism also shows in the extensive research dedicated to this problem.<sup>1-7</sup> The purpose of this Letter is to introduce a broadband semiconductor saturable absorber that can be used as a KLM starting mechanism.

Previously, weak RPM has been used as a continuous starting mechanism for a femtosecond KLM Ti:sapphire laser.<sup>1,3</sup> With RPM a semiconductor saturable absorber inside a coupled cavity strongly mode locks solid-state lasers, and by reducing the coupling to the main cavity (i.e., weak RPM) it continuously starts KLM operation without perturbing the stable femtosecond mode-locked operation. However, one major drawback for tunable solid-state lasers was the demonstrated tuning range of only 30 nm. Because the semiconductor nonlinearity is based on a near-

band-gap nonlinearity it was not obvious how to extend the tunability much further.

Here we present a solution in which we extend the tunability to more than 100 nm using a band-gap-engineered low-temperature molecular-beam-epitaxy (MBE)-grown bulk AlGaAs semiconductor saturable absorber. To obtain such a broadband operation, the absorption edge of the saturable absorber has been artificially broadened by continuously reducing the Al concentration during the MBE growth. We use a picosecond RPM Ti:sapphire laser with no dispersion compensation (Fig. 1) to determine the bandwidth of this broadband saturable absorber. We remain in the picosecond pulse regime to ensure that RPM, and therefore the resonant nonlinearity of the broadband semiconductor absorber, is the dominant mode-locking mechanism and that KLM operation is negligible. The extension to a femtosecond KLM Ti:sapphire laser has been discussed previously.<sup>1,3</sup>

Semiconductor saturable absorbers are attractive because they can cover band gaps from the visible to the infrared, allow for integration, and support an all-solid-state laser technology. The low-temperature MBE-grown saturable absorber produces a nonlinear reflector with a fast component (sub-100-fs) that is due to intraband carrier thermalization and a slower component (a few picoseconds) that is due to carrier

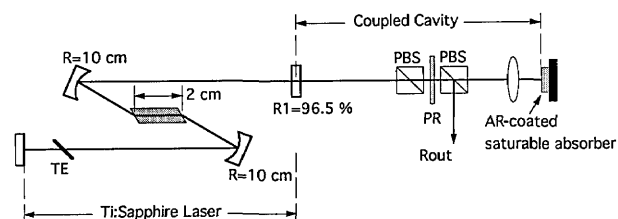


Fig. 1. RPM Ti:sapphire laser setup. PBS's, polarizing beam splitters; PR, polarization rotator; TE, birefringent tuning element; AR, antireflection.

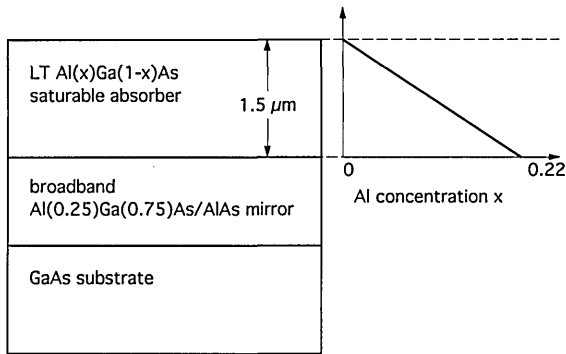


Fig. 2. Broadband AlGaAs saturable absorber design.

recombination, which starts and sustains stable mode locking of cw-pumped solid-state lasers.<sup>9,10</sup> The use of a low- $Q$  coupled cavity (RPM) or an intracavity antiresonant Fabry-Perot saturable absorber<sup>10</sup> (A-FPSA) effectively transforms the semiconductor to an absorber with high saturation intensity and low loss. The A-FPSA is an integrated version of RPM (or monolithic RPM) that replaces the external cavity and forms a compact ( $\approx 400 \mu\text{m}$  thick) nonlinear semiconductor mirror. Because this Fabry-Perot saturable absorber is operated at antiresonance the nonlinear mirror has a large free spectral range ( $>100 \text{ nm}$ ), which will allow incorporation of a broadband saturable absorber.

We engineered the broadband saturable absorber as follows: An  $\text{Al}_x\text{Ga}_{1-x}\text{As}$  absorber layer,  $1.5 \mu\text{m}$  thick, is MBE grown at low temperatures ( $300^\circ\text{C}$ ) on top of a broadband AlGaAs/AlAs mirror. During the absorber layer growth the  $x$  composition is continuously reduced from 0.22 to 0 (Fig. 2), which changes the band-gap wavelength from  $723 \text{ nm}$  at  $x = 0.22$  to  $870 \text{ nm}$  at  $x = 0$ . The  $x$  composition of the  $\text{Al}_x\text{Ga}_{1-x}\text{As}$  absorber layer was changed by lowering the temperature of the cell inside the MBE growth chamber. The finished saturable absorber was annealed at  $580^\circ\text{C}$  at an As overpressure for 30 min to increase the carrier lifetime to a few picoseconds. Finally, the absorber was antireflection coated.

The multilayer AlGaAs/AlAs mirror underneath the absorber layer was MBE grown on a GaAs substrate at normal growth temperature. The chosen Al concentration of 0.25 is high enough to prevent any significant absorption in the dielectric mirror but is too high to produce a sufficiently broad high-reflection bandwidth. Therefore, to obtain a 140-nm mirror bandwidth, the mirror consists of two different stacks of multilayer dielectric mirrors, grown on top of each other with overlapping reflection bands.<sup>11</sup> Ideally we would like to have a 100% reflectivity of this mirror. However, because the low- $Q$  coupled cavity is not very sensitive to loss, we limited the number of periods in the mirror as a compromise between maximum reflectivity and MBE growth time. The first stack has 16 periods of  $\text{Al}_{0.25}\text{Ga}_{0.75}\text{As}/\text{AlAs}$  layers designed for a center wavelength of  $836 \text{ nm}$ . The second stack has 18 periods designed for a center wavelength of  $770 \text{ nm}$ . The designed reflectivity of each stack is then  $\approx 98\%$ . To impedance match the two mirror stacks, a low-index AlAs layer, a

quarter-wave thick at  $803 \text{ nm}$ , was grown between the mirror stacks.<sup>11</sup> This prevents a reflection peak at the overlapping wavelength of  $803 \text{ nm}$  and results in smooth wavelength tuning. We verified an  $\approx 140\text{-nm}$  reflectivity bandwidth by measuring the mirror reflectivity after etching away the GaAs substrate [Fig. 3(a), dashed curve].

The measured low-intensity reflectivity [Fig. 3(a), solid curve] shows that the absorption edge is broadened. We observe weak Fabry-Perot fringes because of residual reflection at the antireflection-coated surface. When the absorber is used inside the laser we typically observe a 4-nm red shift of the semiconductor mirror owing to heating introduced by the higher incident laser intensity. For comparison, we show the absorption edge of a low-temperature multiple-quantum-well saturable absorber,  $1 \mu\text{m}$  thick, consisting of 74 periods of 10-nm-wide GaAs quantum wells and 3.5-nm-wide  $\text{Al}_{0.3}\text{Ga}_{0.7}\text{As}$  barriers grown on an  $\text{Al}_{0.11}\text{Ga}_{0.89}\text{As}/\text{AlAs}$  mirror [Fig. 3(b), solid curve].

Figure 1 shows the cavity configuration of the RPM Ti:sapphire laser, which is based on a Coherent standing-wave Ti:sapphire laser (Model 899 LC). To reduce the overall size of the laser system, we used a coupled cavity with half the length of the main cavity, which increases the pulse repetition rate to 192 MHz. A  $10\times$  microscope lens with a long working distance focused the laser beam to an  $\approx 12\text{-}\mu\text{m}$ -diameter beam size at the nonlinear reflector. Inside the coupled

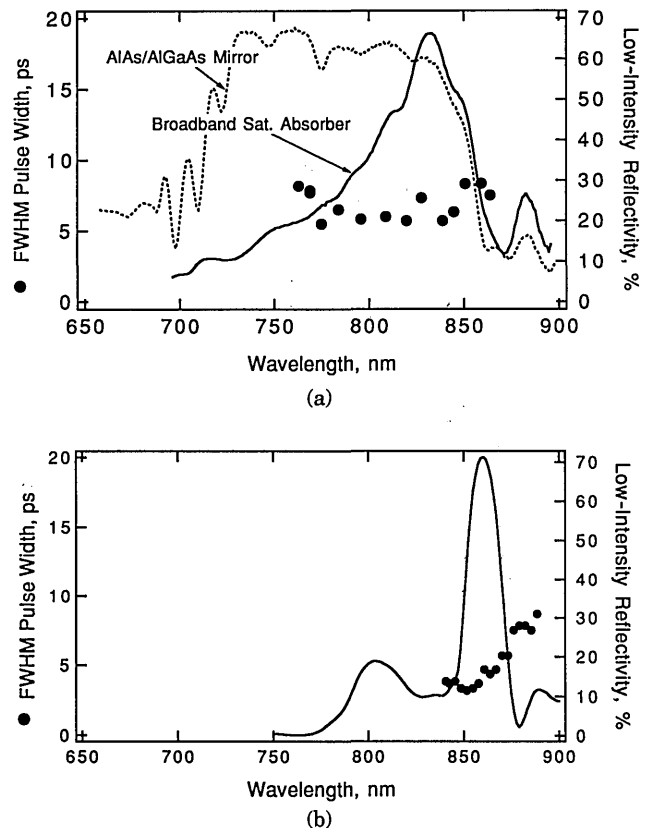


Fig. 3. Low-intensity reflectivity (solid curve) and obtained RPM pulse duration (filled circles) of (a) the low-temperature broadband saturable absorber and (b) the low-temperature multiple-quantum-well saturable absorber. Superimposed in (a) is the reflectivity of the integrated broadband mirror (dashed curve).

cavity, we used a variable output coupler  $R_{\text{out}}$ , formed by two broadband polarizing beam-splitter cubes (PBS) and a broadband polarization rotator (PR). We operated the laser at  $\approx 30\%$  output coupling and at a cavity length detuning of  $\approx -0.3$  mm to obtain self-stabilized RPM without an active cavity length control.<sup>9</sup> The lasing wavelength was controlled by rotating the single-element birefringent tuning element (TE) inside the Ti:sapphire laser.

For the diagnostics we used a real-time non-collinear autocorrelator, a fast photodiode with a sampling scope, and a microwave spectrum analyzer. The stability is good as observed on all the instruments simultaneously. The output power of the Ti:sapphire laser was kept at either 250 or 150 mW constant average output power. This required a slight adjustment of the argon-ion pump power ( $\approx 0.3$  W) over the wavelength tuning range. To maintain stable mode locking and to compensate for the wavelength-dependent absorption in the saturable absorber, we had to decrease the output coupler  $R_{\text{out}}$  (Fig. 2) from 35% at 778 nm to 25% at 867 nm. Even though there is a much larger change in absorption over the full tuning range of the saturable absorber [Fig. 3(a)], the output coupler had to be varied by only a small amount because the effective reflectivity for the laser cavity is strongly reduced by the small coupling strength between the two coupled cavities.<sup>9</sup>

The average pulse duration (assuming a  $\text{sech}^2$  pulse shape) over the tuning range is 6.8 ps with  $\pm 20\%$  maximum pulse-width variations [Fig. 3(a), filled circles]. The tuning bandwidth is 103 nm, which is significant considering the fact that the mode-locking mechanism is still based on a near-band-gap nonlinearity. At the higher power level the tunability is slightly reduced to 97 nm. This reduction can be compensated for with a weaker focusing lens.<sup>9</sup> In comparison, in the case of the low-temperature multiple quantum well, the average pulse width is  $\approx 6$  ps with a large pulse-width variation over a 48-nm tuning range [Fig. 3(b), filled circles], similar to the p-i-n multiple-quantum-well saturable absorber used initially.<sup>12</sup> Previously, we have seen that at wavelengths with longer pulse durations the mode-locking driving force is reduced and is insufficient to start femtosecond KLM operation.<sup>3</sup>

The low-temperature-grown saturable absorbers before annealing had a subpicosecond carrier lifetime. Because the nonlinear reflectivity change is based on absorption bleaching (i.e., the number of photogenerated electrons in the conduction band), a subpicosecond carrier lifetime reduces the number of electrons generated within one mode-locked pulse and therefore the nonlinear reflectivity, which increases the mode-locking buildup time.<sup>13</sup> Therefore, to achieve self-starting mode locking over the full tuning range, we annealed the samples. The annealing increased the carrier lifetime to 6 ps as measured by using the RPM Ti:sapphire laser in a standard noncollinear pump-probe experiment.

In conclusion, we have demonstrated a broadband bulk semiconductor saturable absorber that extended the wavelength tunability of a RPM Ti:sapphire laser to 103 nm. The mode locking is self-starting and stable over the entire tuning range. In addition, the results presented in this Letter demonstrate that a bulk semiconductor with a picosecond carrier lifetime can be used to mode lock solid-state lasers. Previously, we only used multiple-quantum-well structures. The tunability range could potentially be increased by further broadening the absorption edge. For example, the Al concentration can be extended from 0 to 0.45 (limited by the direct band gap), which would broaden the absorption edge to over 250 nm. Such a broadband saturable absorber could be incorporated inside an A-FPSA.<sup>10</sup> The free spectral range of the A-FPSA could be significantly increased by using a selective lift-off technique<sup>14</sup> and a broadband multilayer evaporated dielectric mirror (i.e.,  $\text{TiO}_2/\text{SiO}_2$ ). Such a broadband saturable absorber can be used as an effective starting mechanism for femtosecond KLM operation, where the semiconductor saturable absorber dominates the initial pulse-forming process.<sup>3</sup>

We gratefully thank K. W. Goossen and T. H. Chiu for helpful discussions, G. Doran and D. G. Coult for the AR coating, and T. H. Chiu for annealing the samples.

## References

1. U. Keller, W. H. Knox, and G. W. 'tHooft, *IEEE J. Quantum Electron.* **28**, 2123 (1992).
2. D. E. Spence, P. N. Kean, and W. Sibbett, *Opt. Lett.* **16**, 42 (1991).
3. U. Keller, G. W. 'tHooft, W. H. Knox, and J. E. Cunningham, *Opt. Lett.* **16**, 1022 (1991).
4. N. Sarukura, Y. Ishida, and H. Nakano, *Opt. Lett.* **16**, 153 (1991).
5. D. E. Spence, J. M. Evans, W. E. Sleat, and W. Sibbett, *Opt. Lett.* **16**, 1762 (1991).
6. C. Spielmann, F. Krausz, T. Brabec, E. Wintner, and A. J. Schmidt, *Opt. Lett.* **16**, 1180 (1991).
7. L. Spinelli, B. Couillard, N. Goldblatt, and D. K. Negus, in *Digest of Conference on Lasers and Electro-Optics* (Optical Society of America, Washington, D.C., 1991), paper CPDP7.
8. C.-P. Huang, M. T. Asaki, S. Backus, M. M. Murnane, H. C. Kapteyn, and H. Nathel, *Opt. Lett.* **17**, 1289 (1992).
9. U. Keller, and T. H. Chiu, *IEEE J. Quantum Electron.* **28**, 1710 (1992).
10. U. Keller, D. A. B. Miller, G. D. Boyd, T. H. Chiu, J. F. Ferguson, and M. T. Asom, *Opt. Lett.* **17**, 505 (1992).
11. A. F. Turner and P. W. Baumeister, *Appl. Opt.* **5**, 69 (1966).
12. U. Keller, W. H. Knox, and H. Roskos, *Opt. Lett.* **15**, 1377 (1990).
13. U. Keller, T. H. Chiu, and J. Ferguson, "Self-starting and self-Q-switching dynamics of a passively mode-locked Nd:YLF and a Nd:YAG laser," *Opt. Lett.* (to be published).
14. E. Yablonovitch, T. Gmitter, J. P. Harbison, and R. Bhat, *Appl. Phys. Lett.* **51**, 2222 (1987).